Supplemental Document: Power Diagrams and Sparse Paged Grids for High Resolution Adaptive Liquids

Mridul Aanjaneya, Ming Gao, Haixiang Liu, Christopher Batty and Eftychios Sifakis

Lemma 1. *No face in the power diagram can arise between two cells in the octree that only shared a vertex.*

Proof. Consider the points p_1 and p_2 at the centers of two power cells C_1 and C_2. From the definition of the power diagram, the plane $\mathcal{P}$ between them satisfies the equation,

$$d_1^2 - r_1^2 = d_2^2 - r_2^2 \tag{1}$$

where $d_1 = |p - p_1|$ and $d_2 = |p - p_2|$ are the distances of an arbitrary point p, and r_1, r_2 are the radii of the circumspheres S_1, S_2 for the power cells C_1, C_2. $\mathcal{P}$ is the *secant plane* that passes through the intersection circle of S_1 and S_2. The primal-dual orthogonality property of power diagrams ensures that p_1p_2 is perpendicular to $\mathcal{P}$, let p_0 be the intersection point. It follows that when a face exists between C_1 and C_2 in the power diagram, then $|p_0 - p_1| < r_1$ and $|p_0 - p_2| < r_2$.

Now assume that the octree cells O_1, O_2 centered at the points p_1, p_2 only shared a vertex q. When the radius of each power cell is $\Delta x/\sqrt{3}$ (or $\Delta x/\sqrt{2}$ in 2D), then q lies on both S_1 and S_2. However, $|p_1 - q| = r_1$ and $|p_2 - q| = r_2$, so q also satisfies equation (1), implying that it lies on the plane $\mathcal{P}$. It follows that the plane $\mathcal{P}$ is *tangent* to both S_1 and S_2. Thus, there is no face between C_1 and C_2 in the power diagram. □

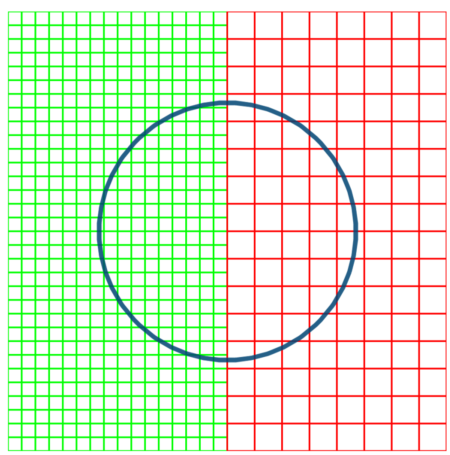

Figure 1: Computational domain for the two dimensional Poisson problem.

Note that the proof for Lemma 1 does not assume any grading restrictions on the octree, suggesting that this property holds in general.

Numerical validation

We now show the numerical convergence of our discretization on some analytic problems. Consider an analytic pressure field satisfying $p = x^2 + y^2 - r^2$ and a level set field $\phi = \sqrt{x^2 + y^2} - r$ in the domain $[-0.5, 0.5] \times [-0.5, 0.5]$, where $r = 0.25$. Regions inside the level set contain pressure degree of freedom, while

Effective resolution	32^2	64^2	128^2	256^2	512^2
L_∞ error	0.000753682	0.000207968	$5.58272e^{-5}$	$1.44169e^{-5}$	$3.68431e^{-6}$
Order of accuracy	–	1.86	1.90	1.95	1.97

Table 1: Convergence results for the two dimensional Poisson problem.

Effective resolution	32^3	64^3	128^3	256^3
L_∞ error	0.00115148	0.00030693	$8.1405e^{-5}$	$2.15657e^{-5}$
Order of accuracy	–	1.91	1.91	1.92

Table 2: Convergence results for the three dimensional Poisson problem.

Effective resolution	32^2	64^2	128^2	256^2	512^2
L_∞ error	0.0159432	0.0100688	0.00494522	0.0024499	0.00121924
Order of accuracy	–	0.58	1.02	1.01	1.01

Table 3: Convergence results for our fast marching scheme in two dimensions.

Effective resolution	32^3	64^3	128^3	256^3	512^3
L_∞ error	0.0227256	0.0138875	0.00731823	0.00342631	0.00187874
Order of accuracy	–	0.71	0.92	1.09	0.87

Table 4: Convergence results for our fast marching scheme in three dimensions.

those outside serve as Dirichlet boundary conditions. Our quadtree has two levels of adaptivity, with fine resolution on one side and coarse on the other (see Figure 1). Table 1 shows the convergence results from our discretization. We similarly consider an analytic pressure field $p = x^2 + y^2 + z^2 - r^2$ and a level set field $\phi = \sqrt{x^2 + y^2 + z^2} - r$ in three dimensions. Table 2 shows the convergence results. As can be seen, our discretization achieves second order accuracy. We also evaluated the order of accuracy of our hybrid fast marching scheme. Table 3 shows the convergence behavior of our method in the two dimensional setting of Figure 1, while Table 4 shows the corresponding behavior in three dimensions.